

Assemblage of Bacterial Saccharic Microfibrils in Sheath Skeleton Formed by Cultured *Leptothrix sp.* Strain OUMS1

Mitsuaki Furutani, Tomoko Suzuki, Hiromichi Ishihara, Hideki Hashimoto, Hitoshi Kunoh and Jun Takada*

Department of Material Chemistry, Graduate School of Natural Science and Technology, Okayama University, Okayama 700-8530, Japan

Abstract

Leptothrix spp., a type of Fe- and Mn-oxidizing bacteria, is characterized by the formation of extracellular Fe- or Mn-encrusted microtubular sheaths in aquatic environments. The sheath matrix is known to be a hybrid of bacterial polymers and aquatic metals and minerals. This study describes the initial phase of assemblage of saccharic microfibrils in the sheath skeleton formed by *Leptothrix sp.* strain OUMS1 in 1–3 day culture investigated using various light and electron microscopic techniques. The negative staining of OUMS1 cells demonstrated a monotrichous polar flagellum and fibrous materials being secreted from the entire cell surface. Specific staining at light microscopic level revealed that viable bacterial cells were involved in the initial development phase of the immature sheath that contained saccharic polymers comprising various sugars. Transmission electron microscopy proved that secretion occurred from the entire cell surface to form membrane-unbound globules within 1 day of culture. After being released from the cell surface, these globules assembled to form the immature fibrous sheath layer away from the cell, resulting in the intervening space between the cell and the layer. It seems likely that secreted globules continuously moved toward the initial immature sheath layer through the intervening space and contributed to thickening of the layer. Alkaline bismuth staining revealed that the globules and the immature sheath materials contain saccharic polymers. By the second day of culture, electron-dense materials containing metals began depositing on fibrous components of the immature sheath layer. Results led us to conclude that the assembly of bacterial saccharic polymers to form the fibrous layer and the subsequent deposition of aquatic metals on the layer constructed the initial frame of the sheath. This new knowledge of the successive steps of sheath development provides deeper insights into the significance of bacterial saccharic polymers in the initial phase of sheath skeleton assembly.

Keywords: *Leptothrix sp.* OUMS1; Sheath formation; Bacterial saccharic polymers; Bacterial exudation; PHA

Abbreviations: TEM: Transmission Electron Microscopy; SEM: Scanning Electron Microscopy; STEM: Scanning Transmission Electron Microscopy; HAADF: High-Angle Annular Dark Field-STEM; EDX: energy dispersive X-ray; SIGP: silicon-iron-glucose-peptone; DIC: Differential Interference Contrast Microscopy; DAPI: 4',6-diamidino-2-phenylindole dihydrochloride; V/D: Viable/Dead; V/C: Viability/Cytotoxicity; FITC: Fluorescein isothiocyanate; Con A: Concanavalin A; LCA: Lens culinaris agglutinin; PNA: Peanut (*Arachis hypogaea*) agglutinin; PHA-E: Phaseolus vulgaris agglutinin E; WGA: Wheat germ agglutinin; PHA: Polyhydroxyalkanoates

Introduction

The Fe/Mn-oxidizing bacteria are known for their ability to form extracellular Fe- or Mn- encrusted structures in aquatic environments. The Sphaerotilus-Leptothrix group of bacteria is characterized by the formation of a tubular sheath often surrounded by a slime layer that is closely connected to the Fe-accumulating and Mn-oxidizing capacities of the organisms. These properties lead to the formation and accumulation of large amounts of ferric and manganese oxides that are characteristic of most *Leptothrix spp.*[1]. Chan et al. reported that organic polymers could play important roles in ecosystems by accumulating biologically important elements and that microbial polymers could scavenge iron oxide particles and induce crystallization of unexpected phases [2]. Many studies have proved that the sheath matrix of *Leptothrix* is composed of a complicated hybrid of bacterial exopolymers and aquatic metals [3-7]. The significance of bacterial secretion in sheath formation has been broadly recognized, but the initial mechanisms of sheath development are not well understood. In a schematic model of the architecture and potential function of the sheath in *Leptothrix cholodnii* SP-6 [4], it was emphasized that

secretion of metal-oxidizing factors, such as metal oxidases and polysaccharides, from the bacterial cells may promote the initial phase of sheath formation [8]. These studies led us to recognize the importance of secretions from bacterial cells and to examine the initial steps from the cellular secretion of materials to the assembly of the immature sheath skeleton, focusing on the flow of saccharic polymers in the cultured *Leptothrix sp.* strain OUMS1 [9] (hereafter referred to as OUMS1). The techniques applied in this study included specific staining at light microscopic level, transmission electron microscopy (TEM), scanning electron microscopy (SEM), scanning transmission electron microscopy (STEM), high-angle annular dark field (HAADF)-STEM, and energy dispersive X-ray spectroscopy (EDX).

Materials and Methods

Sample and culturing

OUMS1 (NITE BP-860) was isolated from flocculent ochreous deposits in the biological freshwater purification plant in Joyo City, Kyoto Prefecture, Japan and stocked in a –80°C freezer [9]. Using the

*Corresponding author: Jun Takada, Department of Material Chemistry, Graduate School of Natural Science and Technology, Okayama University, 3-1-1 Tsushima-naka, Kita-ku, Okayama, 700-8530, Japan, Tel: +81-86-251-8107; Fax: +81-86-251-8087; E-mail: mjtakada@cc.okayama-u.ac.jp

Received August 02, 2011; Accepted October 13, 2011; Published October 16, 2011

Citation: Furutani M, Suzuki T, Ishihara H, Hashimoto H, Kunoh H, et al. (2011) Assemblage of Bacterial Saccharic Microfibrils in Sheath Skeleton Formed by Cultured *Leptothrix sp.* Strain OUMS1. J Marine Sci Res Development S5:001. doi:10.4172/2155-9910.S5-001

Copyright: © 2011 Furutani M, et al. This is an open-access article distributed under the terms of the Creative Commons Attribution License, which permits unrestricted use, distribution, and reproduction in any medium, provided the original author and source are credited.

method described by Sawayama et al. [9], OUMS1 recovered from the frozen stock was cultured in a silicon-iron-glucose-peptone (SIGP) [9] liquid medium with 3 Fe plates (10 × 10 × 1.2 mm³; 99.9% purity; Kojundo Chemical Laboratory, Saitama, Japan) at 20°C on a rotary shaker at 70 rpm for 1–3 and 14 days. Sheath-associated bacterial mats were gently scraped from the surface of the Fe plates and subjected to microscopic observation.

Light microscopy

The collected samples were washed repeatedly with sterilized ultrapure water by centrifugation and subjected to the following specific staining and differential interference contrast (DIC) microscopy.

DAPI staining of bacterial DNA: The specimens were stained with 4',6-diamidino-2-phenylindole dihydrochloride n-hydrate (DAPI, WAKO Chemicals, Japan). The sample suspension (200 µl) in eppendorf tubes were centrifuged at 2,300 × g for 3 min. One milliliter of 1/15 M potassium phosphate buffer (pH 7.4) was added to the precipitate, followed by vortexing and further centrifugation. The resulting precipitate was treated with 20 µl of 5 mM DAPI in the dark at room temperature for 1h. After washing as above, the specimen was mounted with a small aliquote of glycerin on a glass slide and was subjected to fluorescent microscopy (BX51, Olympus) using a U-MWU2 dichroic mirror unit (330–360 nm excitation filter and 430 nm emission wavelengths).

Viable/dead (V/D) bacterial staining: The specimen was resuspended in an Eppendorf tube with 0.85% NaCl and stained with a bacterial viability kit (LIVE/DEAD® BacLight™, L7007, Molecular Probes, Eugene, OR, U.S.A) by following the manufacturer's protocol (hereafter referred to as L/D staining). One milliliter of the specimen suspension was mixed with 3 µl of component A [300 µl of a mixture of SYTO® 9 dye (1.67 mM) and propidium iodide (1.67 mM) in DMSO] and incubated at room temperature in the dark for 15 min. A small drop of the stained specimen was observed by fluorescent microscopy using a U-MWIB3 dichroic mirror unit (460–490 nm excitation filter and 520 nm emission wavelengths).

A similar viability assay was performed using the viability/cytotoxicity assay (V/C assay) kit for viable and dead bacterial cells (No. 30027, BIOTIUM Inc., Hayward, CA, U.S.A). The manufacturer's protocol and the microscopy conditions were almost the same as those for the above-mentioned V/D staining, except for the initial mixing of the components.

As a negative control for both staining procedures, the cells killed by 1h pre-treatment in 70% ethanol were stained similarly as mentioned above.

Fluorescein isothiocyanate (FITC)-conjugated lectin reaction for specific saccharic components: To examine the presence of specific sugars in the cells and the associated sheaths, the sample suspension (200 µl) was mixed independently with 500 µl of each of the FITC-conjugated lectins, concanavalin A (Con A), *Lens culinaris* agglutinin (LCA), peanut (*Arachis hypogaea*) agglutinin (PNA), *Phaseolus vulgaris* agglutinin E (PHA-E), and wheat germ agglutinin (WGA) (10 µg/ml each), in eppendorf tubes and reacted at room temperature for 30 min. A small aliquote of the reaction mixture was dropped onto clean glass slides and mixed with a small volume of glycerol. The glass-covered specimens were subjected to fluorescent microscopy using a U-MNIBA3 dichroic mirror unit (470–490 nm excitation filter and 520 nm emission wavelengths). A control experiment was conducted to ensure that the test FITC-conjugated lectins bound only to their

respective haptens present in the bacterium-associated structures. In this experiment, each lectin (10 µg/ml) was mixed for 1 h with 200 mM solution of the known competitive hapten carbohydrate (glucose or mannose for Con A and LCA; galactose for PNA; N-acetyl-D-galactosamine for PHA-E, and N-acetyl-D-glucosamine for WGA).

Electron microscopy

a) Transmission electron microscopy:

i) Preparation of ultrathin sections: The specimen was collected by centrifugation and fixed with a mixture of 2.5% glutaraldehyde, 1% OsO₄, and 4.5% sucrose in 100 mM cacodylate buffer (pH 7.0) on ice for 2h and then embedded in 2% agar. Small pieces of the washed agar block were dehydrated in a graded series of ethanol and again embedded in Quetol 651 resin mixture (Nisshin EM, Tokyo, Japan). Ultrathin sections were stained with uranyl acetate and lead solution and then observed by TEM (H-7500, Hitachi, Tokyo, Japan) operated at an accelerating voltage of 80 kV.

ii) Negative staining of bacterial cells: OUMS1 was cultured on SIGP agar medium at 20°C for 3 days. The cells scraped from the medium surface were suspended in ultrapure water. The cells collected by centrifugation were resuspended in 300 µl of 1% phosphotungstic acid. A small aliquote was dropped onto formvar-coated grids and gently soaked up with a small piece of filter paper. This serial step was repeated 3–4 times. The air-dried grids were subjected to TEM observation.

iii) Alkaline bismuth staining for the detection of constitutive saccharic component: Following the carbohydrate-staining technique devised by Park et al. [10], the ultrathin sections on copper grids were exposed to 40-fold-diluted alkaline Bi stock solution for 30 min at 40°C. The alkaline Bi stock solution was composed of 10% sodium hydroxide, 4% potassium sodium tartrate, and 2% Bi subnitrate in ultrapure water [10]. After repeated washing with ultrapure water, the grids were subjected to TEM observation.

b) Scanning electron microscopy: The collected samples were washed repeatedly with sterilized ultrapure water and vacuum-dried. The dried samples were mounted onto an aluminum specimen stub and vacuum-dried for 30 min. After Pt-coating the specimen was subjected to observation with a scanning electron microscope (S-4300, Hitachi, Tokyo, Japan).

c) HAADF-STEM imaging and elemental mapping: The Bi- and U/Pb-stained ultrathin sections on copper grids were first covered with a formvar film by a routine method and coated with carbon to increase the tolerance of the specimen to an intense electron beam. HAADF-STEM and EDX detectors attached to a JEOL JEM-2100F (accelerating voltage; 200 kV) transmission electron microscope were used for HAADF-STEM imaging and mapping of Bi and Pb respectively. Bright field STEM images were also obtained for reference.

Results and Discussion

Sawayama et al. [9] reported that in artificial culture medium OUMS1 produces microtubular sheaths morphologically similar to those formed by other species and strains of *Leptothrix* in nature (hereafter referred to as natural sheaths). Although our primary interest in this study was the initial phase of formation of the uniquely shaped sheaths, we first attempted to briefly investigate the 14-day-old culture. As described earlier [9], cultivation of OUMS1 in SIGP medium results in a remarkable increase in the number of fluffy, ocherous deposits. Many aged hollow tubular structures (hereafter referred to as cultured

sheaths) were observed in the deposits on the surface of the Fe plate using SEM (Figure 1A). A high-power image of the cut plane of a sheath shows more detail (Figure 1B) of the fluffy outer and the globular inner surfaces of the sheath wall.

The outer coats of the natural and cultured sheaths were distinct in appearance. The outer coat of the natural sheaths of *Leptothrix* spp. seemed tightly netted with agglutinated thin fibrils [7,11], whereas the outer coat of the cultured sheaths was composed of loosely-woven thin and assembled thick fibrils. In contrast, the globular inner surfaces of both sheaths were similar. As evident in Figure 1B, the entire wall of sheaths was 0.3–0.4 μm thick and seemed homogeneous. As illustrated in Figure 1B (inset), developmentally bushy fibrils surrounded the thick electron-dense wall of the sheath.

These results sparked our keen interest in the significance of bacterial saccharic polymers in the initial step of sheath construction. In the 3-day-old culture, negative staining successfully showed two dividing cells surrounded by electron-dense materials. Figure 1C shows a monotrichous, polar, and curvy flagellum arising from the left side of the cell, which is consistent with the earlier description of OUMS1 morphology [9], and suggested that flagellum locomotion may be significant in this strain, in contrast to the unknown locomotion mechanism in *Leptothrix ochracea* [1]. Another high-power negative staining image (Figure 1D) revealed numerous electron-lucent curvy fibrils arising from the entire surface of a single cell. Such fibrils were much thicker than known pili and with secretion products from the cell surface. To our knowledge, this image is the first clear image showing a material release from *Leptothrix* cells by electron microscopy.

The initial phase of sheath formation was observed by DIC microscopy and DAPI and V/D staining, V/C assay, and lectin staining for the first 3 days of culture. At day 1, many single cells and linked cells (Figure 2A, D) were observed in the culture. A faint film was distinguishable only around some linked cells by DIC microscopy. At day 2, many linked cells had been enclosed in a distinct film (Figure 2B, E), representing the formation of the immature sheath. The adjacent cells within the immature sheaths were not always tightly connected, and thus intercellular spaces were often observed (Figure 2B, E, arrow). At day 3, a larger number of longer and thicker film-coated, lined cells were observed (Figure 2C, F). Under the current filter conditions of

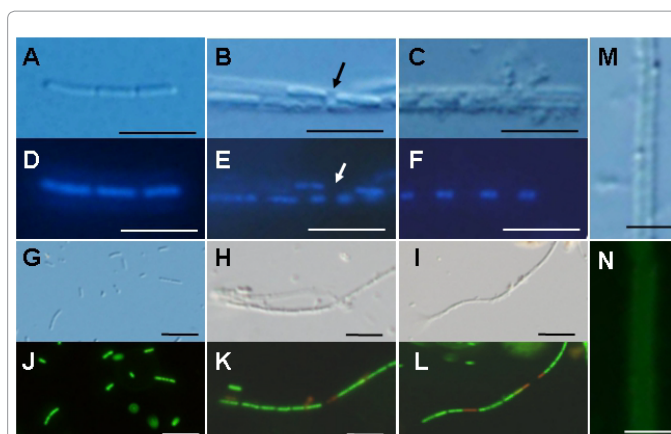
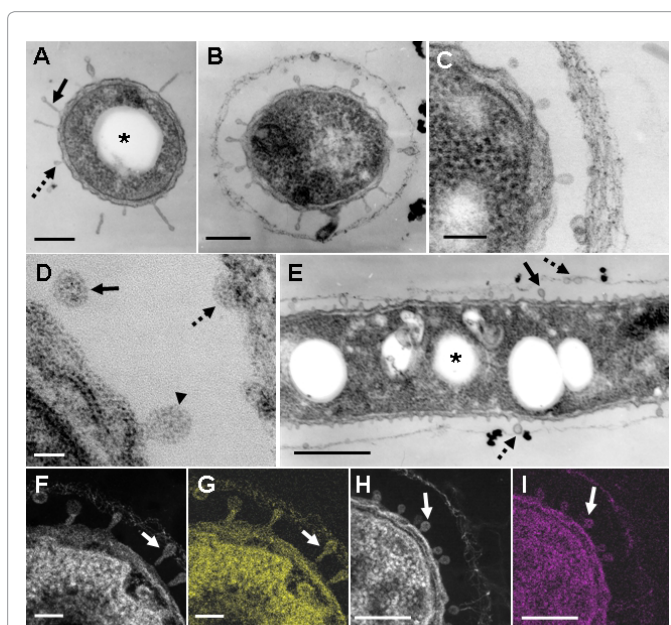


Figure 2: DIC microscopy images and specific staining of bacterial cells in 1–3-day cultures. (A, D) A line of cells lacking sheath and its positive response to DAPI staining of the cells at day 1. (B, E) Two lines of cells surrounded by an immature sheath and their response to DAPI staining at day 2. (C, F) An arrow shows the intercellular gap. A line of cells surrounded by a relatively thick sheath and its response to DAPI staining at day 3. Note that separate cells are enclosed in the sheath. (G–I) V/D staining of cells in 1- to 3-day cultures in this order. (G–I) DIC microscopy images and (J–L) fluorescence images. (M, N) DIC microscopy image and positive response to PHA-E lectin, respectively, at day 2. Scale bar: (A–F, M and N) 5 μm, (J–L) 10 μm.



*: PHA

Figure 3: TEM, STEM and HAADF-STEM images and elemental maps in ultrathin sections prepared at day 1. (A) TEM image of a sheath-free cell having globular and/or slender forms of exudates from the cell surface. (B) TEM image of a cell surrounded by a thin immature sheath layer. (C) Enlarged TEM image of the loosely-woven fibrils in an immature sheath in Bi-stained section. (D) A high-power STEM image of membrane-unbound globular exudates. (E) TEM image of a longitudinal section of the cell surrounded by a thin immature sheath layer. (A, D, E) Arrows indicate the exudates from the bacterial surface in various states. (F, G) HAADF-STEM image of Bi-stained cross-section of the cell and Bi distribution map. (H, I) HAADF-STEM image of U/Pb-stained cross section of the cell and Pb distribution map. (F–I) White arrow indicates the protuberances. Scale bar: (A, B, E,) 500 nm, (C, F–I,) 100 nm, (D) 20 nm.

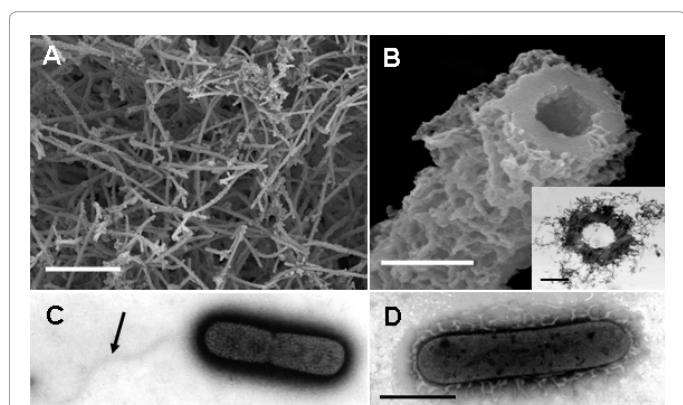


Figure 1: Aged sheaths in 2-week culture and bacterial cells in 1-day culture. (A) SEM image of numerous tubular sheaths formed on a Fe plate surface in 2-week culture. (B) Enlarged SEM image of an aged sheath and TEM image of its cross-section (inset). (C) Negative staining image of a dividing cell with a monotrichous polar flagellum (arrow) in 3-day culture. (D) Negative staining image of a cell secreting materials of electron-lucent fibrous appearance in 3-day culture. Scale bar: (A) 50 μm, (B–D) 1 μm.

fluorescent microscopy for L/D staining and V/C assay, viable bacteria with intact cell membranes stained fluorescent green, whereas those with damaged membranes stained red. During the 3 days, most linked cells in the sheath responded fluorescent green (Figure 2G-L). At days 2 and 3, however, fluorescent red cells coexisted with green cells within the same line of cells (Figure 2K, L), suggesting that some cells died in the immature sheath. There was no regularity in the appearance of red cells in the enclosed cell lines. Free single red cells were often observed in the 1–3-day cultures. Moreover, some of the free or enclosed cells were yellowish, which suggested at least a partial loss of integrity of their cell membranes. The cells responded similarly to both assays (V/C data not shown). The pre-killed cells stained red in both assays. The specific staining showed that viable bacteria are involved in at least the initial phase of sheath assembly.

Lawrence et al. [12] detected polysaccharides composed of various sugars in an exopolymeric matrix of microbial biofilm collected from river water using a variety of lectins. Figure 2M and N illustrate DIC microscopy image and positive PHA-E lectin response (specifically bound to N-acetyl-D-galactosamine) of the same immature sheath observed at day 3. Although the degree of fluorescence intensity varied depending on the lectins, as Chan et al. reported in the lectin responses of *Mariprofundus* stalks [13], the immature sheath surrounding the linked cells responded positively to all tested lectins, irrespective of culture days, which provided evidence that glucose, mannose (Con A and LCA), galactose (PNA), and N-acetyl-D-galactosamine (PHA-E) and -glucosamine (WGA) were at least partially contained in the immature sheaths as the saccharic polymer components. It was confirmed in the control assays that pre-treatment of each lectin with the respective competitive hapten carbohydrate caused the absence or reduction of fluorescence in the immature sheath.

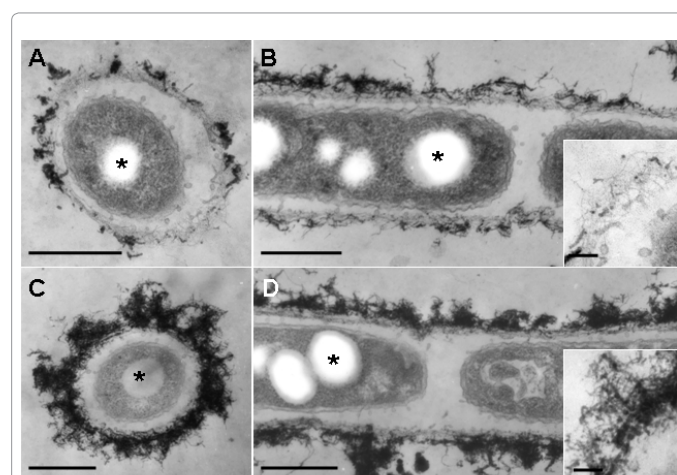
All these observations demonstrate that (i) viable cells release polymers from the entire cell surface and are involved in the primitive phase of sheath development, (ii) linked cells are enclosed in the immature sheath layer, and (iii) this layer contains saccharic polymers comprising various sugars. Currently, it is uncertain whether single cells divide within the immature sheath after enclosing or linked cells are enclosed prior to cell division.

In a review by Ghiorse [3], a TEM image of a thin-sectioned cell of *Leptothrix* sp. shows protuberances originating from the cell envelope in contact with the electron-dense fibrillar sheath material. In addition, he described the presence of acidic extracellular polymers in the protuberances by positive staining with ruthenium red. TEM observations in this study supported his description. At day 1, some cells were free of the immature sheath material (Figure 3A), while others were surrounded by a thin film across the electron-lucent space (Figure 3B-E). Interestingly, many protuberances were secreted from the entire cell envelope of the cells (Figure 3A-C). In a free single cell, some protuberances were of a globular shape (Figure 3A, dotted arrow), while others had a slender form projected from the cell envelope (Figure 3A, solid arrow). It is most likely that such protuberances correspond to electron-lucent fibrils originating from the cell envelope in the negative staining image (Figure 1D). Furthermore, the protuberances released from the mother cells attached to the inner surface of the surrounding film (Figure 3E, dotted arrow). The immature sheath is an assembly of parallel-woven long fibers (Figure 3C). The mechanisms by which these fibrous forms are constructed remain unsolved at present. Details of the protuberances are shown in a high-power STEM image (Figure 3D). Some protuberances were connected to the cell envelope (Figure 3D, arrowhead), whereas others were disconnected (Figure

3D, solid arrow). Moreover, some released protuberances were in contact with the thin film of the immature sheath (Figure 3D, dotted arrow). It is evident that the protuberances were not membrane-encompassed vesicles (Figure 3D), suggesting that they were not formed by the outgrowth of the cell envelope but by the extrusion of saccharic polymers from the cell. HAADF-STEM imaging and elemental mapping proved that the bacterial cell, protuberances, and immature sheath materials bound to Bi (Figure 3F, G) and Pb (Figure 3H, I). The alkaline Bi applied to thin sections binds to constituent carbohydrate [10] and the lead staining is considered to depend upon the formation of a stable lead-glucose complex through hydrogen bond [14]. Accordingly, considering the above lectin responses, Figure 3F–I evidently indicate that the positively-responding structures contain saccharic polymers.

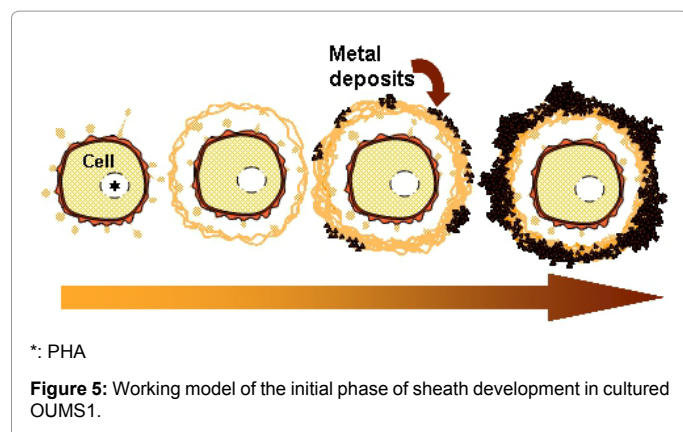
At day 2, the features of the immature sheath changed markedly when compared with day 1. Almost all linked cells were surrounded by a thin layer or relatively thick layer of electron-dense deposits. Many protuberances were still secreted from the cell surface (Figure 4A). The immature sheath layer became apparently thicker than that observed at day 1 (Figure 4A). Electron-dense fibrous materials deposited at the surface of the sheath layer (Figure 4A, B). As indicated in an enlarged image (Figure 4B, inset), the electron-dense fibrils loosely assembled with some deposits. A separate EDX mapping study [9] showed that such deposits contained Fe, P, Si, and other minor elements. At day 3, the electron-dense surface deposits assembled more prominently compared with day 2 (Figure 4C, D). As illustrated in Figure 4D (inset), electron-dense materials deposited in almost all fibrils at the surface layer.

These consecutive observations led us to assume that the thin immature sheath was assembled by the gradual transfer and accumulation of the saccharic polymer-containing protuberances from



*: PHA. Scale bar: (A-D) 500 nm, (B, D inset) 100 nm.

Figure 4: TEM images of Bi-stained sections of bacterial cells associated with the immature sheath prepared at days 2 and 3. (A) A cross-section of the cell associated with an immature fibrous sheath having electron-dense metal deposits on the outer surface (day 2). (B) A longitudinal section of the cells associated with an immature fibrous sheath with a high electron density attributable to a heavy deposition of metals (day 2). Details of assemblage of microfibrils are shown in inset. (C) A cross-section of the cell associated with an immature fibrous sheath with a heavily electron-dense fibrous outer surface (day 3). (D) A longitudinal section of the linked cells surrounded by an immature sheath with a heavily electron-dense fibrous outer surface (day 3). Details of the electron-dense fibrous assembly are shown in inset.



the cell surfaces through the intervening space between the cell and the layer within 1 day of culture and that deposition of aquatic metal and/or mineral ions on the primitive fibrous layer led to the maturation of the sheath by day 2 of culture.

Some fine fibrous and/or globular structures existed in this space (Figure 3B-E and 4A-D), suggesting that this space was composed of a liquid phase and was not air-filled. This space could play a significant role in the continuous transfer of bacterial saccharic polymers and other secretion products from the cell to the sheath layer, leading to the maturation of the sheath layer as seen in Figure 1B.

The conspicuous inclusion of the bacterial cells attracted our attention. Almost all cells had several electron-lucent inclusions that lacked a definite boundary composed of a unit membrane (Figure 3A, E and 4A-D, star), as similarly as those in earlier TEM images of *Leptothrix* cells [3,4,9,15]. This inclusion probably corresponds to polyhydroxyalkanoates (PHA) which is commonly considered as a storage material of bacterial cells [16-18]. Other papers generally recognize that Fe- and Mn-oxidizing bacteria acquire electron energy by oxidizing Fe²⁺ and Mn²⁺ in aquatic environments as energy sources for their survival [3]. However, the habitual presence of PHA-like structure in the cells led us to consider the possible use of this material as another energy source for cell growth besides electron generation by metal oxidation.

The current observations are summarized in the putative schematic model on the initial phase of sheath development (Figure 5). Chan et al. [2] considered that organic polymers could act as templates that serve as a pattern for the production of a second structure (sheath). Our study failed to solve an interesting question about how the globular secretion products convert to fibrous architectures in the immature sheath layer. The current study successfully provided deeper insights into the initial phase of sheath development, however, the mechanism by which aquatic metals deposit on such fibers leading to the aged form of the sheath remains unsolved.

Acknowledgments

This study was financially supported by a Special Grant for Education and Research (2008-2013) and a Grant-in-Aid for Research Activity Start-up (No. 22860040, 2010 and 2011) from the Ministry of Education, Culture, Sports, Science, and Technology, Japan (for J. T. and H. H., respectively), and a Grant-in-Aid from the Yakumo Foundation for Environmental Science (for H.H. and T. S.).

References

1. Van Veen WL, Mulder EG, Deinema MH (1978) The *Sphaerotilus-Leptothrix* group of bacteria. Microbiol Rev 42: 329-356.
2. Chan CS, Stasio GD, Welch SA, Girasole M, Frazer BH, Nesterova MV, Fakra S, Branfield JF (2004) Microbial polysaccharides template assembly of nanocrystal fibers. Science 303: 1656-1658.
3. Ghiorse WC (1984) Biology of iron- and manganese-depositing bacteria. Annu Rev Microbiol 38: 515-550.
4. Emerson D, Ghiorse WC (1993a) Ultrastructure and chemical composition of the sheath of *Leptothrix discophora* SP-6. J Bacteriol 175: 7808-7818.
5. Emerson D, Ghiorse WC (1993b) Role of disulfide bonds in maintaining the structural integrity of the sheath of *Leptothrix discophora* SP-6. J Bacteriol 175: 7819-7827.
6. Takeda M, Makita H, Ohno K, Nakahara Y, Koizumi J (2005) Structural analysis of the sheath of a sheathed bacterium, *Leptothrix cholodnii*. Int'l J Biol Macromol 37: 92-98.
7. Sakai T, Miyazaki Y, Murakami A, Sakamoto N, Ema T, et al. (2010) Chemical modification of biogenous iron oxide to create an excellent enzyme scaffold. Org Biomol Chem 8: 336-338.
8. Spring S (2006) The genera *Leptothrix* and *Sphaerotilus*. Prokaryotes 5: 758-777.
9. Sawayama M, Suzuki T, Hashimoto H, Kasai T, Furutani M, et al. (2011) Isolation of a *Leptothrix* strain, OUMS1, from ochreous deposits in groundwater. Curr Microbiol 63: 173-180.
10. Park P, Ohno T, Kato-Kikuchi H, Miki H (1987) Alkaline bismuth stain a tracer for Golgi vesicles of plant cells. Stain Technol 62: 253-256.
11. Hashimoto H, Yokoyama S, Asaoka H, Kusano Y, Ikeda Y, et al. (2006) Characteristics of hollow microtubes consisting of amorphous iron oxide nanoparticles produced by iron oxidizing bacteria, *Leptothrix ochracea*. J Magn Mater 310: 2405-2407.
12. Lawrence JR, Swerhone GD, Leppard GG, Araki T, Zhang X, et al. (2003) Scanning transmission X-ray, laser scanning, and transmission electron microscopy mapping of the exopolymeric matrix of microbial biofilms. Appl Environ Microbiol 69: 5543-5554.
13. Chan CS, Farka SC, Emerson D, Fleming EJ, Edwards KJ (2011) Lithotrophic iron-oxidizing bacteria produce organic stalks to control mineral growth: implications for biosignature formation. ISME J 5: 717-727.
14. Reynolds ES (1963) The use of lead citrate at high pH as an electron-opaque stain in electron microscopy. J Cell Biol 17: 208-212.
15. Emerson D, Ghiorse WC (1992) Isolation, cultural maintenance, and taxonomy of a sheath-forming strain of *Leptothrix discophora* and characterization of manganese-oxidizing activity associated with the sheath. Appl Environ Microbiol 58: 4001-4010.
16. Steinbüchel A (1992) Biodegradable plastics. Curr Opin Biotechnol 3: 291-297.
17. Jendrossek D (2009) Polyhydroxyalkanoate granules are complex subcellular organelles (carbonosomes). J Bacteriol 191: 3195-3202.
18. Mayet C, Dazzi A, Prazeres R, Ortega JM, Jallard D (2010) *In situ* identification and imaging of bacterial polymer nanogranules by infrared nanospectroscopy. Analyst 135: 2540-2545.